STUDY OF MUON BACKGROUNDS IN THE CLIC BEAM DELIVERY SYSTEM

H. Burkhardt, L.Gatignon, A. Latina, D. Schulte, R. Tomas, CERN, Geneva, Switzerland

B. Pilicer *, E.Pilicer, I. Tapan, Uludag University, Bursa, Turkey

Abstract

We describe the detailed modelling of muon background generation and absorption in the CLIC beam delivery system. The majority of the background muons originates in the first stages of halo collimation. We also discuss options to use magnetised cylindrical iron shields to reduce the muon background flux reaching the detector region.

INTRODUCTION

For the Compact Linear Collider (CLIC) project, high energy beam will be transported to the interaction region (IR) by the Beam Delivery System (BDS) [1]. The BDS is 2796 m long and consists of four sections which are diagnostics, energy and betatron collimation and final focus, respectively. The betatron collimation section has horizontal and vertical spoilers ($\sim 1\,X_0$) and absorbers ($\sim 20\,X_0$) to remove halo particles. The interaction of the halo particles with the spoilers and absorbers produces secondary particles including muons. Most of the secondary particles will be absorbed rather locally. High energy muons are not stopped by the absorbers and may reach the experimental detectors at the interaction point. Here we study how the background muon flux to the detector can be reduced using cylindrical magnetized shielding blocks of 5 m or $\sim 300\,X_0$ length. The main processes for muon production are gamma conversion into muon pairs (Bethe-Heitler process, $\gamma e^- \rightarrow \mu^+\mu^- e^-$) and annihilation of positrons with atomic electrons into muon pairs ($e^+e^- \rightarrow \mu^+\mu^-$). For the study described here we use the BDS of the CDR, and include the process of e^+e^- annihilation into hadrons ($e^+e^- \rightarrow$ hadrons) as an additional source for background muons [2]. The description of an earlier study can be found in [3].

MUON PRODUCTION PROCESSES

We use Geant4 (version Geant4.10.01) for the simulation of the interaction of the beam particles and secondary particles with the material in the beam line [4, 5]. The cross sections for the electromagnetic processes which are at the origin of muon production are shown in Fig. 1 as a function of the incoming beam energy, up to 1.5 TeV (maximum beam energy for CLIC).

The kinetic energy of atomic electrons in matter is very small compared to the beam energies considered here. In a very good approximation, we are dealing with the annihilation of high energy positrons with electrons at rest. The
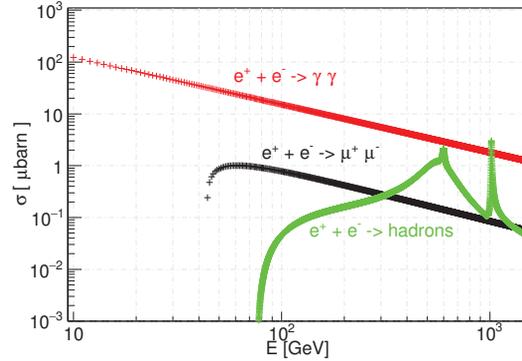
Figure 1: Cross sections for annihilation into two gammas (red markers), $\mu^+\mu^-$ (black markers) and hadrons (green markers) in laboratory frame energy.
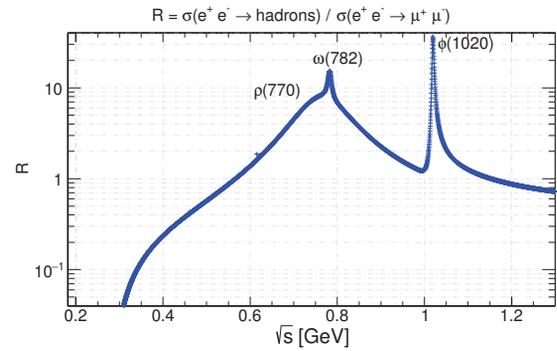

Figure 2: Ratio R = $\sigma_{e^+e^- \rightarrow hadrons}/\sigma_{e^+e^- \rightarrow \mu^+\mu^-}$ as function of the center of mass energy frame.

relevant centre of mass energy for the annihilation of high energy positrons of energy E_{beam} with electron of mass m_e at rest is $\sqrt{2 \cdot m_e \cdot E_{beam}}$, or 1.24 GeV at 1.5 TeV beam energy [2]. The ratio R of hadron to muon cross sections for the relevant centre-of-mass energy range is shown in Fig. 2. The peaks in the cross section for annihilation to hadrons correspond to the masses of vector resonances. The first two peaks visible at around 600 GeV beam energy correspond to $\rho(770)$ and $\omega(782)$. The peak around 1 TeV beam energy corresponds to the $\phi(1020)$. At these beam energies, the muon production by collimation of high energy positrons will be increased compared to muon background by electron collimation.

The hadrons produced in e^+e^- annihilation at these energies are : K^+K^-, $K_S K_L$, $\pi^+\pi^-$, $\pi^+\pi^-\pi^0$, $\pi^0\gamma$, $\eta\gamma$. The charged pions, kaons and the K_L are relatively long lived and will only rarely produce background muons by hadron decay. High energy photons produced in the decay of the
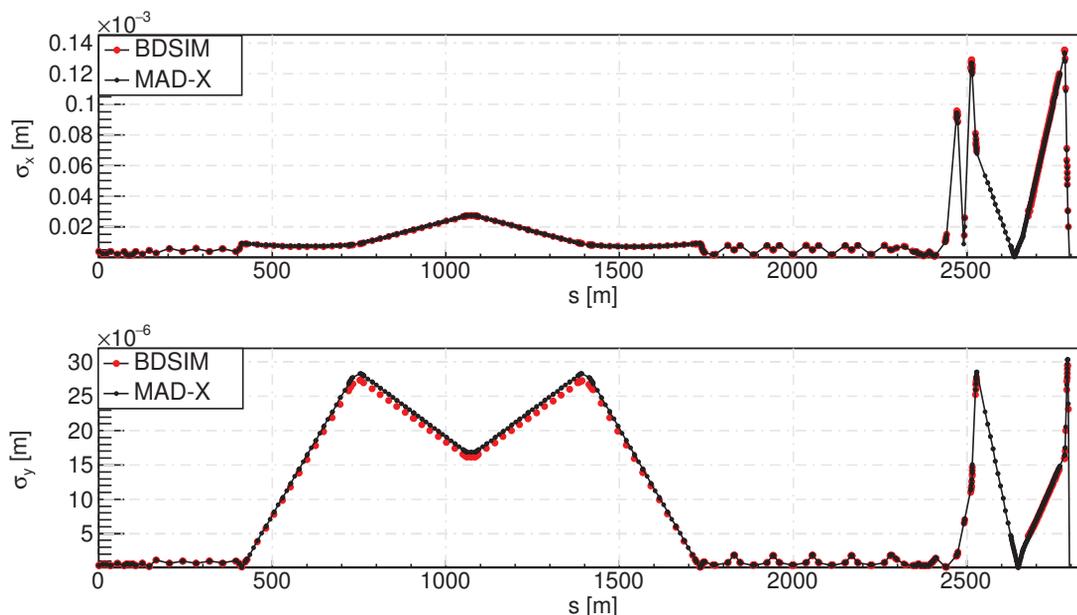
Figure 3: Comparison of horizontal and vertical RMS beam sizes by MAD-X and BDSIM along the whole BDS.

short lived π^0 ($\tau_{\pi^0} = 8.52 \times 10^{-17} s$), η ($\tau_\eta = 5.0 \times 10^{-19} s$) and K_S ($\tau_{K_S} = 8.95 \times 10^{-11} s$) mesons will add to muon production by gamma conversion.

MODELLING BEAM DELIVERY SYSTEM AND MUON BACKGROUND WITH BDSIM

We use the Beam Delivery Simulation (BDSIM) code [6], which is a Geant4 / C++ based software, to trace beam particles through the BDS. The whole BDS geometry was built using input written in GMAD format as required for BDSIM, based on MAD-X input with additional geometry information. The geometry was tested by tracking 10^4 1.5 TeV e^- primary beam particles through the whole line using BDSIM version v0.62. The beam sizes obtained in the simulation agree well with the expectations from MAD-X as can be seen in Fig. 3.

The betatron collimation section is designed to collimate away halo particles. The halo particles which hit the spoilers will be scattered and lose energy by Bremsstrahlung. The scattered beam-halo particles and Bremsstrahlung photons will typically impact on the downstream absorbers. The scattered beam particles, Bremsstrahlung photons and e^+e^- pairs generated in the electromagnetic cascades are absorbed rather locally. Any high energy muons produced in the processes discussed in the previous section, can instead travel rather far and potentially reach the detector region.

To better understand the production and absorption process, we performed simulations in several steps. As a first step we studied halo particles which hit the first spoiler close to the edge. The program was run for 10^4 1.5 TeV e^- particles by setting a 10^4 bias factor for muon production processes and annihilation into hadron process. To limit CPU time, only secondaries above a minimum threshold of 1 GeV were followed up. The tunnel radius has been taken as 3 m.

The primary beam halo particles mainly generate muons at the absorbers, see Fig. 4. Only a small fraction of the muons is produced by interaction of secondary particles in the long dipole section in the final focus. The dominant production process is gamma conversion into muon pairs. Only a small fraction of the muons originates in the decay of hadrons, as can be seen from Fig. 4.

Many of the muons produced will leave the beam pipe at large angles and will be lost in the surrounding tunnel walls. Only a smaller fraction which however increases with muon energy, will reach the detector region. The energy spectrum of the muons extends up to nearly the beam energy. The highest energy observed here was 97% of the beam energy. Most of the muon energies are below 200 GeV. High energy muons can penetrate long heavy shielding. Muons have a relatively long lifetime ($\sim 2.2\ \mu s$ at rest) and will only rarely decay before they reach the detector region.

A magnetized shielding can be an effective option to deflect muons away from the beam line into the tunnel wall. We have started to simulate magnetized shielding for cylindrical elements made of iron. We simulate cylindrical shielding of 5 m length, an inner radius of 1 cm, and an outer radius of 50 cm, using toroidal magnetic B_ϕ field, where ϕ is the azimuthal angle around the beam axis. They are much longer and heavier than the spoilers and absorbers for betatron collimation, we will also refer to these cylinders as *massive shielding*. We position them in existing drift spaces in the betatron collimation section of the BDS, without any need for modifications to existing active beam elements. The length of the shielding will not be sufficient to stop the muons. The purpose of the magnetic shielding is rather to decrease the muon flux into the detector by bending the muons away from the centre of the beam line.
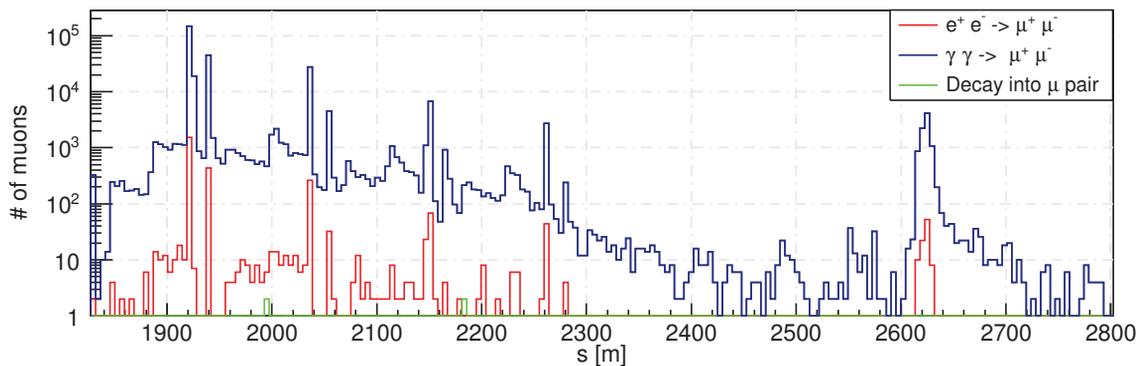
Figure 4: Origin of muons along the BDS from primary electrons hitting to the first spoiler in betatron collimation section.
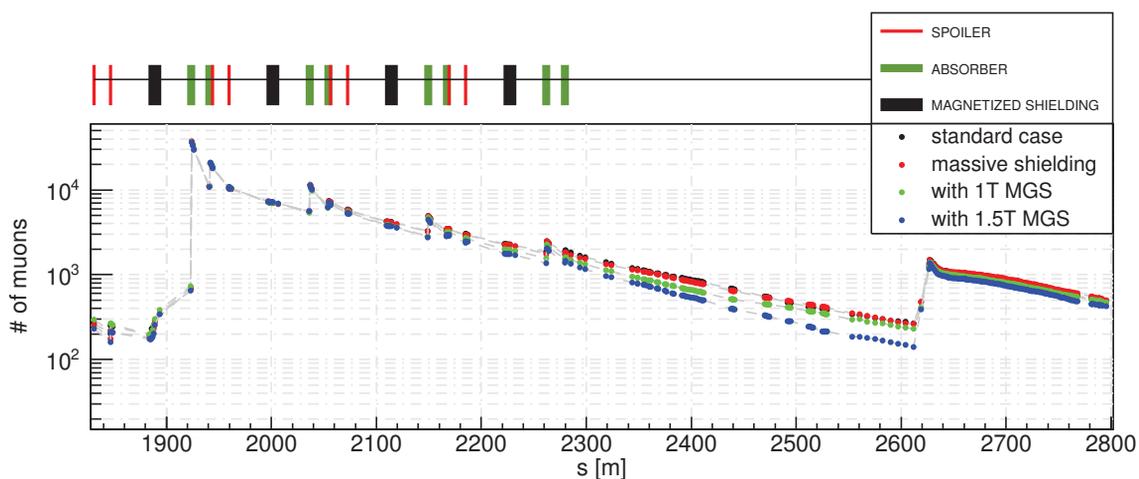

Figure 5: Effect of magnetized shieldings to the muon flux in betatron collimation section.

We use the 34.5 m long drift spaces between the horizontal spoilers (XSP) and horizontal absorbers (XAB) as locations for magnetized spoilers. The positions are sketched on the top of Fig. 5. We performed simulations starting from the beginning of the betatron collimation (at the first vertical spoiler YSP1) and extending up to the IP for four different scenarios. The first scenario, referred to as *standard case*, is the simulation of the BDS from the CLIC conceptual design without any addition of shielding.

For the second scenario we have added the massive shielding blocks, but without any magnetic field. The third and fourth scenario are with massive magnetized shielding with peak fields of 1 T and 1.5 T respectively. The results are illustrated in Fig. 5. Each point indicates the number of muons, which are arrive at the sample plane of an element. The increase at around 2640 m corresponds to muon production by particles hitting aperture limits in the BDS.

We see that the dominant muon flux originates in the betatron collimation section and that is this flux is reduced by the shielding. We also see that the shielding effects increases with the magnetic field.

SUMMARY

We have set up a detailed simulation of muon production and shielding for the BDS of the CLIC conceptual design using BDSIM. We have also used GEANT4 to directly study the individual contributions of the underlying muon production processes. As the next step we plan to simulate the full BDS with combined momentum and betatron collimation and to perform an overall optimisation of the muon flux reduction to the detector by optimisation of collimation depths and shielding positions and fields.

REFERENCES

[1] M. Aicheler, P. Burrows, M. Draper, T. Garvey, P. Lebrun, K. Peach, N. Phinney, H. Schmickler, D. Schulte and N. Toge edited, "A Multi-TeV linear collider based on CLIC technology: CLIC Conceptual Design Report", 2012.

[2] A. Bogdanov, H. Burkhardt *et al.*, "Geant4 Simulation of High Energy Muon Interactions" ,IEEE Transactions on Nuclear Science, Vol.53, 2 April 2006.

[3] L. Deacon *et al.*, Muon Background Reduction in CLIC, arXiv:1202.6628

[4] S. Agostinelli *et al.*, "Geant4-a simulation toolkit", Nuclear Instruments and Methods in Physics Research A 506 (2003) 250-303.

[5] J. Allison *et al.*, "Geant4 developments and applications", IEEE Transactions on Nuclear Science 53 No. 1 (2006) 270-278.

[6] BDSIM,
`http://twiki.ph.rhul.ac.uk/twiki/bin/view/PP/JAI/BdSim`